Textural analysis of skin cancer tumors on OCT images

D. S. Raupov[a], O. O. Myakinin[a], I. A. Bratchenko[a], A. G. Khramov[a]

[a] *Samara National Research University, 443086, 34 Moskovskoye Shosse, Samara, Russia*

Abstract

In this paper, we propose a report about our two years investigations in skin cancer texture analysis on OCT images from different tissues. We suggest method compiled from Haralick texture features, fractal dimension, complex directional field features and Markov random field method. Additionally, boosting has been used for the quality enhancing of the diagnosis method. We obtained precision about 90% for two classes cases and about 75% for four classes case.

Keywords: Markov random fields; textural analysis; complex directional field; fractal analysis; optical coherence tomography; Haralick features; boosting; skin cancer

1. Introduction

Optical Coherence Tomography (OCT) is a great tool for contactless nondestructive study of optically inhomogeneous mediums [1]. Recently, effective application of OCT was confirmed in various directions of clinical practice such as gastroenterology, urology, dermatology, gynecology, ophthalmology, otolaryngology, stomatology and others [2, 3]. OCT has a position as a non-invasive method of visualization of inner structure of optically heterogeneous objects based on a principle of low-coherence interferometry using near infrared range (0.75–1.3 μm) as light source. OCT visualizes an inner microstructure of skin down to 2 mm with space resolution 10-15 μm without human tissue blasting [4]. Moreover, OCT is a very high-speed diagnosis tool. Up to 6 volumes per second (with lateral resolution 500×500 px) may be obtained in case of 1.5 MHz Swept-Source laser using [5], which means OCT may be used for quasi real-time imaging.

Optical coherence tomography is usually employed for the measurement of structural changes of tissue. The possibility of OCT in detecting changes using Haralick's texture features, fractal dimension and complex directional field from different tissues is investigated in this paper.

Any coherent technic implies speckle noise impact. In general case, the noise can be removed by digital filter from final OCT volume after a mandatory PC processing. On the 2D slice of tissue volume in vertical (B-scan) or horizontal (C-scan) planes, it is possible to see dynamics of anisotropic growth of healthy skin and malicious tissue. It is just an image in terms of Digital Image Processing and the denoising may be implemented as a general image processing filter [6, 7]. We used an interval type-II fuzzy anisotropic diffusion algorithm [8, 9] for speckle noise reduction in OCT images for this research as more reliable for processing on OCT images [10, 11].

Haralick texture features are evaluated in different directions for comparing effectivity of proposed features and amplification sensitivity and specificity. These quickly computable features contain useful information for categorizing, classifying diagnostic images as B-scans. However, in biology and medicine, the shapes of structures such as molecules, cells, tissues and organs also play an important role in the diagnosis of diseased tissue [11, 12]. Fractal dimension could also distinguish the structural changes of tissue. Quantitative mensuration of the fractal dimension could be an efficient concept to differ tumor tissue from normal healthy tissue [13-17]. So the structural changes in fractal dimension may give further information observing cellular layers and injury in skin pathology. Besides, the using of the OCT techniques contributes to the application of fractal analysis in the diagnostics of skin cancer. The bizarre skin tissue could be revealed by accomplishment of fractal analysis for certain biological structures in OCT images. Thus, fractal analysis with the OCT imaging techniques could give an efficient diagnostic methodology to classify tumors as BCC and MM [18]. Also it can be used for differentiation between nevus and healthy skin probes. Usually we can simplify dependencies of tissue states each from other by suggestion that each pixel depends from only its neighbors. So computing Markov random fields' features can provide us useful information about nature of tumor.

We included a method of directional field to this features list to improve the characteristics' quality of tumor recognition. Malignant tissue growth anysotropically, which means that it may be presented by the complex directional field calculated from a C-scan. General features like variance and correlation could be used for dividing scans with tumor and healthy probes. A basic idea of a directional field application is an attempt to analyze the directions of anisotropic growth of malicious skin and possibility of tissue further development. High relevant results on quasiregular structures such as interferograms, fingerprints, crystallograms and many others show us its universality [19]. The complex form provides more evaluation precision and a relationship between a directional field and a weight function. The C-scan analyzing gives us an ability to appreciate other planes of spreading pathology on the cellular layers.

Unfortunately, we also should take into account additional a priory information about preliminary diagnosis when we use textural features for common dividing between two classes (MM or BCC, MM or nevus etc.). Thus, it could be a big challenge

for general practitioner. So, it is very important to have a universal classifier for accurate definition between many tumor classes. A priory information is also required for this case, but preliminary diagnosis could be much less accurate. The boosting is used in this work with aim to generalize all textural features, enhance diagnosis quality and receive classifier for discriminating between 4 classes (MM, BCC, nevus or healthy skin). Additionally, we tested ANN as an alternative method of machine learning to create a linear combination of described textural features for increasing sensitivity and specificity.

The institutional Review Board of Samara National Research University and Samara State Medical University approved the study protocol. This research adhered to the tenets set forth in the Declaration of Helsinki. Informed consent of each subject was obtained.

2. OCT-setup scheme

The OCT system (Figure 1) consists of a broadband superluminescent laser diode (840±25 nm wavelength range, 20 mW output power) at the source end, Michelson interferometer with 50/50 split ratio to the sample and reference arms and a spectrometer at the detector end. The spectrometer includes a diffraction grating (1200 grooves/mm) and a CCD line scan camera (4096 pixel resolution, 29.3 kHz line rate). The interference signal from the sample and the reference arms of the Michelson interferometer is revealed by the spectrometer and processed by an image acquisition card (NI-IMAQ PCI-1428). Depth profile (A-line) is received by transforming the interference signal revealed by the IMAQ into linear k-space [20].

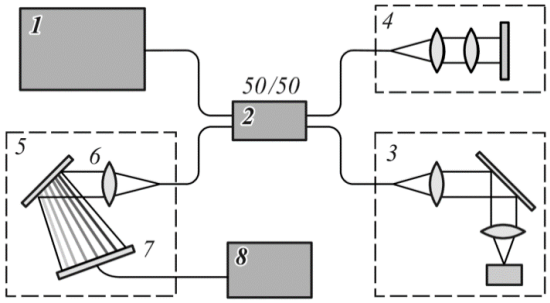

Fig. 1. Spectral domain OCT scheme: 1 – broadband source, 2 – 50/50 beamsplitter, 3 – sample arm, 4 – reference arm, 5 – spectrometer with grating 6 and CCD camera 7, 8 – computer with IMAQ.

3. Methods

3.1. Textural features

For evaluating Haralick features, a gray-level co-occurrence matrix (GLCM) from an image should be calculated. GLCM is based on frequency evaluating of a pixel with gray-level value i horizontally (vertically, diagonally) connected to a pixel with the value j. Each element (i, j) in GLCM specifies the number of times that the pixel with value i occurred horizontally adjacent to a pixel with value j [10, 11, 21, 22].

The most popular algorithm for computing the fractal dimension of one dimensional and two dimensional data is the box counting, method originally developed by Voss [23]. In this method, the fractal surface is covered with a grid of n-dimensional boxes or hyper-cubes with side length, ε and counting the number of boxes that contains a part of the fractal $N(\varepsilon)$. As for signals, the grid consists of squares and for images, the grid consists of cubes. The fractal surface is covered with boxes of recursively different sizes. An input signal with N elements or an image of size $N * N$ is used as input where N is a power of 2 [10, 24].

$$D_{bc} = \frac{log\, N(\varepsilon)}{log\frac{1}{\varepsilon}}. \quad (1)$$

Other method for counting fractal dimension is differential box-counting method [11],[25]. It is possible to estimate D**,** the fractal dimension, from the least square linear fit of $\log N_r$ against $\log(1/r)$ [26]. Also we used power-spectrum method for counting fractal dimension [27]. The merits of this approach are it is generalizable, potentially more accurate and the computation of D_F is based on an explicit formula [25].

Complex directional field (CDF) defines as:

$$\dot{\varphi}(x, y) = w(x, y)\, exp\big(i2\varphi(x, y)\big), \quad (2)$$

where $\varphi(x, y)$ is a directional field; $w(x, y)$ is a weight function (WF), has a physical meaning as reliability of directional field in the point [10], [11], [28].

A Markov random field, Markov network or undirected graphical model is a graphical model in which a set of random variables have a Markov property described by an undirected graph [29]. Connection of nodes with each other is defined by

localities system as $N = \{N_s | s \in S\}$, where N_s is a neighbors set of node s, S is finite set of nodes. Localities system has property $s \notin N_s$. Random field is called as Markov random field in relation to localities system, if for all $z_i \in Z$ next condition is realized: $P(z_i | z_{S/i}) = P(z_i | z_{N_i})$, where $Z = \{Z_1, \dots, Z_m\}$ – random field, z_i – values of random variables Z_i. We use suggestion that OCT-image may be presented as a Markov random field, so pixel intensity depends only from intensities of neighboring pixels. Non-causal locality is used [30]. We estimated autocorrelation function (AF) as:

$$R(x,y) = \sum^{1}_{\substack{i=-1 \\ I(x+i,y+j)\in N_{x,y}}} \sum^{1}_{\substack{j=-1 \\ I(x+i,y+j)\in N_{x,y}}} I(x,y)I(x+i,y+j). \quad (3)$$

Then we found variation and mean value for using them as textural features [10, 11].

3.2. Boosting

Despite the possible good results of classifiers, it is always possible to improve them by linear combination. In our case we use boosting [31]. The task of precedents learning is considered. $\langle X, Y, y^*, X^l \rangle$, where X – space of objects; $y^*: X \to Y$ – unknown target dependence; $X^l = (x_1, \dots, x_l)$ – is a learning selection; $Y^l = (y_1, \dots, y_l)$ is a vector of answers on learning objects $y_i = y^*(x_i)$. It is needed to build an algorithm: $X \to Y$, that approximated target dependence y^* on all set X [32].

The task of classification on two classes is considered, $Y^l = \{-1, +1\}$. We suggest that solution rule is fixed,

$C(b) = sign(b)$.

Base algorithms return answers -1, 0, +1. Answer $b_t(x) = 0$ means that base algorithm b_t refused from classification object x and answer $b_t(x)$ don't use in composition. Finding algorithm composition has look [33]:

$$a(x) = C\left(F\left(b_1(x), \dots, b_T(x)\right)\right) = sign\left(\sum_{t=1}^{T} a_t b_t(x)\right), x \in X. \quad (4)$$

This paper uses conjugate AdaBoost [34] algorithm for tissues discrimination (tumor, norma; MM, nevus, BCC or healthy skin) quality assessment. The boosting for B-scans uses 10 corresponding parameters as fractal dimensions (FD), counted by 1D-box-counting method (with standard deviation(SD)), 2D-differential box counting method and 2D-power spectrum method, Haralick features (contrast, correlation, homogeneity, energy) and Markov random fields features (variance and mean of autocorrelation function estimation). For C-scans complex directional features (field variance and weight function variance) are used, the maximum quantity of trees [35] was 200.

Table 1. Statistical characteristics of separation tissues by utilized features

		Tissues		**Precision**	**Quantity**	**Type**
Category of feature	**Name of feature**	**Tissue1**	**Tissue2**	**(sensitivity-specificity)**	**(images)**	**(B/C-scan)**
Haralick	Contrast—Correlation	MM	Healthy Skin	88%—92,8%	42/42(84)	B
Haralick	Correlation—Homogeneity	MM	Healthy Skin	88%—95,2%	42/42(84)	B
MRF	AF variance—AF mean	MM	Healthy Skin	92,8%—95,2%	42/42(84)	B
MRF	AF variance—AF mean	MM	BCC	90,4%—83,3%	42/42(84)	B
CDF	WF variance—CDF variance	Nevus	Healthy Skin	97,5%—83,7%	80/80(160)	C
CDF	WF variance—CDF variance	BCC	Nevus	100%-97,5%	80/80(160)	C
CDF	WF variance—CDF variance	MM	BCC	91,5%—100%	80/80(160)	C
Neural networks	Scaled conjugate gradient backpropogation	Tumor	Norma	86,9%—89,3%	84/84(168)	B
Neural networks	Scaled conjugate gradient backpropogation	Tumor	Norma	73,8%—85%	160/160(320)	C
Fractal	SD—FD	Tumor	Norma	70%—71%	42/84(126)	B
Boosting	AdaBoost	MM, BCC	Nevus, Healthy Skin	75%	42/42/42/42(168)	B

4. Results and Discussion

The anisotropic algorithm was used for denoising. Then images are processed by four methods: Haralick's features, fractal analysis, Markov random fields features (for B-scans) and complex directional field features (for C-scans). This paper uses scaled conjugate gradient backpropagation [36] based artificial neural network (ANN) for tissues discrimination (tumor, norm; MM, nevus, BCC or healthy skin) quality assessment. The ANN is trained in MATLAB using 10 corresponding parameters for

B-scans as fractal dimensions, counted by 1D-box-counting method (with standard deviation), 2D-differential box counting method and 2D-power spectrum method, Haralick features (contrast, correlation, homogeneity, energy) and Markov random fields features (variance and mean of autocorrelation function estimation) . The quantity of hidden layers is 10. For C-scans complex directional features (field variance and weight function variance) were used, the quantity of hidden layers was 20.All results are presented in Table 1.

So after that we can say that all methodologies show good results in classifying melanoma from healthy skin. Boosting and neural networks improve significantly all results for other classifications cases. If we compare boosting and neural networks, then we reveal that ANN shows sensitivity and specificity higher than boosting on same set of B-scans. But boosting let us to divide between four classes (MM, BCC, nevus and healthy skin), but not between 2 classes as other classifiers (for example, Tumor (BCC+MM) and Norma (Nevus + Healthy Skin). So we receive more universal classifier that can be used with high precision without waiting histological data for diagnostics.

5. Conclusion

In summary, we have described a methodology to calculate the textural features from OCT images for classifying the MM, BCC and pigment nevi in this paper. The early results presented have shown that the boosting is more universal for classifying than common textural features or neural networks. Future studies are needed to determine the accuracy, repeatability and full capability of this methodology of many-classes classification with more OCT images.

Acknowledgements

This research was supported by the Ministry of Education and Science of the Russian Federation. Authors are thankful to Dr. Wei Gao from Ningbo University of Technology for Matlab code providing for denoising and fractal dimension calculating.

References

[1] Huang, D. Optical coherence tomography / D. Huang, E.A Swanson, C.P. Lin, J.S. Schuman, W.G. Stinson, W. Chang, M. R Hee, T. Flotte, K. Gregory, C. A. Puliafito, J. G. Fujimoto // Science. – 1991. – Vol. 254(5035). – P. 1178-1181.

[2] Fercher, A. F. Optical coherence tomography–principles and applications / A.F. Fercher, W. Drexler, C.K. Hitzenberger, T. Lasser // Rep.Prog.Phys. – 2003. – Vol. 66. – P.239-303.

[3] Sergeev, A. M. Optical tomography of biotissues past, present and future / A.M. Sergeev, L.S. Dolin, D.N. Reitze // Optics&Photonics News. – 2001. – Vol. 12. – P. 28-35.

[4] Genina, E. A. Liver images contrasting in optical coherence tomography with help of nanoparticles / E.A. Genina, S.A. Kinder, A.N. Baschkatov, V.V. Tuchin // Proceedings of Saratov University. – 2011. – Vol. 11(2). – P. 10-13.

[5] Wang, S. Direct four-dimensional structural and functional imaging of cardiovascular dynamics in mouse embryos with 1.5 MHz optical coherence tomography / S. Wang, M. Singh, A.L. Lopez, C. Wu, R. Raghunathan, A. Schill, J. Li, K.V. Larin, I.V. Larina // Opt. Lett. – 2015. – Vol. 40. – P. 4791-4794.

[6] Zakharov, V. P. Increasing the information content of optical coherence tomography skin pathology detection / V.P. Zakharov, K. Larin, I.A. Bratchenko // Proceedings of SSAU . – 2011. – Vol. 26. – P. 232-239.

[7] Zakharov, V. P. Complex optical characterization of mesh implants and encapsulation area / I.A. Bratchenko, V.I. Belokonev, D.V. Kornilin, O.O. Myakinin // J. Innov. Opt. Health Sci. – 2013. – Vol. 6. – 1350007.

[8] Puvanathasan, P. Interval type-II fuzzy anisotropic diffusion algorithm for speckle noise reduction in optical coherence tomography images / P. Puvanathasan, K. Bizheva // Optics Express. – 2009. – Vol. 17(2). – P.733-746.

[9] Tizhoosh, H. Image thresholding using type II fuzzy sets // Pattern Recognition. – 2005. – Vol. 38. – P.2363-2372.

[10] Raupov, D.S. Skin cancer texture analysis of OCT images based on Haralick, fractal dimension and the complex directional field features / D.S. Raupov, O.O. Myakinin, I.A. Bratchenko, D.V. Kornilin, V.P. Zakharov, A.G. Khramov // Proc. SPIE. – 2016. –Vol. 9887. – 98873F.

[11] Wojtkowski, M. High-speed optical coherence tomography: basics and applications. // Applied Optics. – 2010. – Vol. 49(16). – P.30-61.

[12] Forsea, A. M. Clinical application of optical coherence tomography for the imaging of non-melanocytic cutaneous tumors: a pilot multi-modal study / A.M. Forsea, E.M. Carstea, L. Ghervase, C. Giurcaneanu, G. Pavelescu // Journal of medicine and life – 2010. – Vol. 3(4). – P.381-389.

[13] Sarkar, N. An efficient approach to estimate fractal dimension of textural images // Pattern Recognition. – 1992. – Vol. 25(9). – P. 1035-1041.

[14] Huang, J. Fractal image analysis: application to the topography of Oregon and synthetic images / J. Huang, D. Turcotte //J. Opt. Soc. Am. – 1990. – Vol. 7(6). – P. 1124-1130.

[15] Flueraru, C. Added soft tissue contrast using signal attenuation and the fractal dimension for optical coherence tomography images of porcine arterial tissue / C. Flueraru, D.P. Popescu, Y.Mao, S. Chang, M.G. Sowa //Physics in Medicine and Biology. – 2010. – Vol. 55(8). – P. 2317-2331.

[16] Sullivan, A. C., Fractal analysis for classification of breast carcinoma in optical coherence tomography// Journal of Biomedical Optics. – 2013. – Vol. 16(6). – 066010.

[17] Gao, W. Improving the quantitative assessment of intraretinal features by determining both structural and optical properties of the retinal tissue with optical coherence tomography // Ph.D. thesis. – 2012.

[18] Gao, W. Medical images classification for skin cancer using quantitative image features with optical coherence tomography / W. Gao, V.P. Zakharov, O.O. Myakinin, I.A. Bratchenko, D.N. Artemyev, D.V. Kornilin // Journal of Innovative Optical Health Sciences.– 2016. – Vol. 9(2). – 1650003.

[19] Soifer, V.A. Methods of image computer processing / Moscow: Physmathlit , 2003. – P.459-523.

[20] Myakinin, O. O. A complex noise reduction method for improving visualization of SD-OCT skin biomedical images / V.P. Zakharov, I.A. Bratchenko, D.V. Kornilin, A.G. Khramov // Proc. SPIE. – 2014. – Vol. 9129. – 91292Y.

[21] Haralick, R.M. Textural features for image classification / R.M. Haralick, K. Shanmugam, I. Dinshtein // IEEE Trans. Syst. Man Cybern. – 2010. – Vol. 3(6). – P. 610-621.

[22] Haralick, R. M., Computer and Robot Vision: Vol. 1 / R.M. Haralick, L.G. Shapiro. — Addison-Wesley, 1992.—P. 459-460.

[23] Voss, R. F. Random fractal forgeries in: Fundamental Algorithms for Computer Graphics (editor R.A. Earnshaw)/Berlin: Springer-Verlag, 1985— P.805-835.

[24] Annadhason, A. Methods of Fractal Dimension Computation // IRACST. – 2012. – Vol. 2(1). – P. 166-169.

[25] Sarkar, N. An Efficient Differential Box-Counting Approach to Compute Fractal Dimension of Image / N. Sarkar, B.B. Chaudhuri // IEEE Trans. Syst. Man Cybern. – 1994. – Vol. 24(1). – P. 115-120.

[26] Florindo, J. B. Fractal Descriptors in the Fourier Domain Applied to Color Texture Analysis / Florindo, J. B., O.M. Bruno //Chaos – 2011. – Vol. 21(4). – 043112.
[27] Ahammer, H. Higuchi Dimension of Digital Images // PLoS ONE 6(9), e0119394 (2011). – 2011. – Vol. 6(9). – E0119394.
[28] Ilyasova, N. U. Numerical methods and algorithms of building of directional fields in quasiperiodic structures. /N.U. Ilyasova, A.V. Ustinov, A.G. Khramov // Computer Optics – 1998. – Vol. 18. – P. 150-164.
[29] Winkler, G. Image Analysis, Random Fields and Dynamic Monte Carlo Methods / Verlag: Springer, 1995.
[30] Plastinin, A. I. A model of Markov random field in texture image synthesis and analysis / A.I. Plastinin, A.V. Kupriyanov, A. V. // Proceedings of Samara State Aerospace University. – 2008. – Vol. 2. – P. 252-257.
[31] Schapire, R.E. Boosting the margin: A new explanation for the effectiveness of voting methods // Annals of Statistics. – 1991. – Vol. 26(5). – P. 1651-1686.
[32] Vorontsov, K.V. About the problem-oriented bases optimization of recognition problem //Computational Mathematics and Mathematical Physics. – 1998. – Vol. 38(5). – P. 870-880.
[33] Vorontsov, K.V. Optimization methods for linear and monotone correction in the algebraic approach to the recognition problem // Computational Mathematics and Mathematical Physics. – 2000. – Vol. 40(1). – P. 166-176.
[34] Freund, Y. A Decision-Theoretic Generalization of On-Line Learning and an Application to Boosting / Y.A. Freund, R.E. Schapire // J. of Computer and System Sciences. – 1997. – Vol. 55. – P. 119-139.
[35] Breinman, L. Classification and Regression Trees / Boca Raton: Chapman&Hall, 1983.
[36] Moller, M.F. A Scaled Conjugate Gradient Algorithm for Fast Supervised Learning // Neural Networks. – 1993. – Vol. 6. – P. 525-533.